Author's version
accepted for publication in IEEE/ASME Transactions on Mechatronics
doi: 10.1109/TMECH.2016.2603601.

Directional Singularity-Robust Torque Control for Gyroscopic Actuators

Andrew Berry, Daniel Lemus, Robert Babuška *Member, IEEE*, and Heike Vallery *Member, IEEE*

***Abstract*—Gyroscopic actuation is appealing for wearable applications due to its ability to impart free moments on a body without exoskeletal structures on the joints. We recently proposed an unobtrusive balancing aid consisting of multiple parallel-mounted control moment gyroscopes (CMGs) contained within a backpack-like orthopedic corset. Using conventional CMG control techniques, geometric singularities result in a number of performance issues, including either unintended oscillations or freezing of the gimbals at certain alignments, which are typically mitigated by the addition of redundant actuators or by allowing errors in the generated moment; however, because of the minimalistic design of the proposed device and focus on accurate moment tracking, a new methodology is required.**

In this paper, a control scheme is proposed for non-redundant CMG systems in which oscillations at saturated states are avoided and all remaining singularities are efficiently escaped by exploiting the system geometry; due to its use of classification-specific singularity proximity measures that account for the command moment orientation, it is named the *directional singularity-robust* (DSR) control law. The performance of this control law is assessed in both simulations and hardware testing. The proposed method is suitable for a wide range of CMG systems, including both balancing and aerospace applications.

***Index Terms*—control moment gyroscope (CMG), torque control, fall prevention, wearable robotics.**

I. Introduction

In the past several years, parallel studies in humanoid robotics and human rehabilitation technology have, on a number of occasions, advocated using momentum exchange devices (MEDs) to solve the problem of bipedal balancing. These actuators, examples of which include reaction wheels, momentum wheels, and control moment gyroscopes, have the desirable ability of imparting a free moment on a body without necessitating contact with an inertial frame; a recent high-profile example employing reaction/momentum wheels is the Cubli balancing robot [1]. For the design of human balancing aids, MEDs provide an attractive alternative to bulky exoskeletons on the legs. Like a reaction wheel, a control moment gyroscope (CMG) consists of a rotating flywheel or rotor, but the rate of rotation is typically much higher and the mode of operation is fundamentally different: rather than change the spin rate of the rotor to generate a moment, rotation of an outer gimbal (Fig. 1) reorients the rotor and produces a significantly larger gyroscopic moment. Because the generated gyroscopic moment is orthogonal to the gimbal and rotor spin axes, it is applied directly to the gimbal bearings, rather than the rotor or gimbal motors; the implication of this is that, for a relatively small gimbal motor torque, a considerably larger output is possible. Exploiting this *torque amplification effect*, a device can be constructed with smaller, less powerful motors better suited to a wearable application.

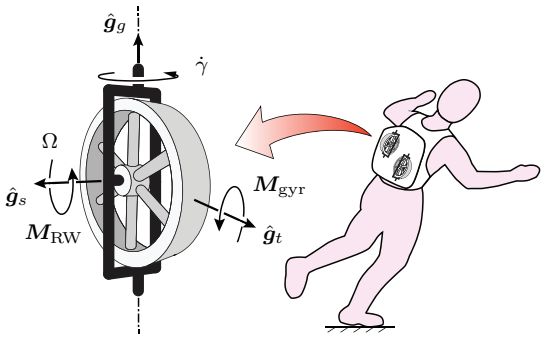

Fig. 1. Schematic of a single-gimbal CMG showing the orientations of the gyroscopic moment ($\boldsymbol{M}_{\mathrm{gyr}}$) and the reaction wheel moment ($\boldsymbol{M}_{\mathrm{RW}}$) exerted on the device in the case of variable flywheel speed. The gimbal-fixed frame $\{\hat{\boldsymbol{g}}_s, \hat{\boldsymbol{g}}_t, \hat{\boldsymbol{g}}_g\}$ is oriented such that $\hat{\boldsymbol{g}}_s \in \mathbb{R}^{3\times 1}$ aligned with the rotor spin axis, $\hat{\boldsymbol{g}}_g \in \mathbb{R}^{3\times 1}$ with the gimbal axis, and $\hat{\boldsymbol{g}}_t \in \mathbb{R}^{3\times 1}$ with the transverse axis. The rotor and gimbal angular velocities are denoted by Ω and $\dot{\gamma}$, respectively.

Although other MEDs had previously been proposed for human balance assistance devices (e.g. [2]), we described first a device utilizing CMGs and harnessing the above benefits [3]. In this concept, a wearable backpack-like device (Fig. 1) would contain multiple lightweight CMGs capable of imparting a moment on the torso to provide balance assistance in any fall direction. This concept was elaborated upon by Matsuzaki and Fujimoto [4] and a simplified prototype was constructed by Chiu and Goswami [5], consisting of a symmetric pair of CMGs with a mechanical constraint to synchronize gimbal motions and aid balancing in the sagittal plane only; however, despite this progress, the control of such nonlinear actuators remains challenging for wearable applications.

One such challenge is the handling of geometric singularities in the gimbal angles, whereby the individual CMG moment vectors $\boldsymbol{M}_{\mathrm{gyr},i}$ align such that their span loses rank, thereby disrupting moment generation in certain directions and incurring excessive gimbal rates. Singularity-robust CMG control techniques have been extensively documented for certain actuator layouts in the context of spacecraft attitude control [6], but little detailed information is available on other applications, in particular those involving non-redundant actuator arrangements and the balancing of unstable systems;

All authors are with the TU Delft Robotics Institute, Delft University of Technology, Delft, 2628 CD the Netherlands.

H. Vallery is also with the Sensory-Motor Systems Laboratory, ETH Zurich, Zurich, 8092 Switzerland (email: h.vallery@tudelft.nl).

Manuscript received November 4, 2015; accepted for publication August 25, 2016.

nevertheless, the basic solution framework remains similar. A controller for a CMG array generally consists of two (not necessarily distinct) components: an outer feedback law responsible for converting the objective quantity (typically a reference attitude) into a reference moment and compensating for disturbances, and an inner model-based control allocation scheme (often called a *gimbal steering law*) responsible for generating the gimbal and rotor acceleration commands necessary to track this moment. We describe in [7] an exemplary outer control law in the form of a pre-parametrized moment profile, and instead focus here on the latter element.

The control allocation law concerns inversion of the system model to compute the control inputs and must contend with the occurrence of singularities and manage them in such a way that the actuator limitations are respected. If the system is modelled sufficiently well, the gimbal trajectories can be precomputed via optimization or search-based techniques [8]–[10] or calculated in real-time using model-predictive control [11], [12] to minimize the cumulative tracking errors; however, due to the high computational load, inherently unpredictable dynamics of humans, and the corresponding gyroscopic disturbances induced by the body motion, such a strategy is ill-advised for the proposed application. *Instantaneous* methods use only the current system state for control and typically consist of analytical formulations with fixed structure, making use of a particular (net-moment-producing) solution and, if a redundant number of CMGs is available, also a homogeneous (non-net-moment-producing) component. The particular component is typically computed as the Moore-Penrose pseudoinverse of the system Jacobian, yielding the minimum-norm gimbal rates required to track the reference moment, yet on its own it is ineffective at avoiding singularities. The homogeneous component, derived from the nullspace of the Jacobian, can be utilized at or near singular configurations to reorient the gimbals without affecting the net output moment in a procedure known as *null-motion*; singularities may be avoided by driving the system to a desired state [13] or modifying the gimbal trajectory such that either a measure of proximity to singularity is maximized or an arbitrary function of this measure is used to impart a "non-directional" change of trajectory [14]. The availability of such techniques (regardless of their effectiveness) is dependent upon the use of excess CMGs, but, to ensure the mass and volume of our device is suitable for elderly users, it should contain no more actuators than absolutely necessary for balancing in the coronal and sagittal planes; hence, a non-redundant configuration of $N = 2$ CMGs is used and null-motion is not possible. Rather than strive for complete singularity avoidance, an alternative approach is to use only the particular solution but strategically inject moment tracking errors to moderate the gimbal rates while passing directly through the singular configuration. Such methods are based on the solution to the regularized (damped) least-squares problem, which weighs tracking accuracy against gimbal rates. Notable examples are the *singularity-robust* (SR) inverse steering law of Bedrossian [14], adapted from the works of Wampler [15] and Nakamura and Hanafusa [16] in robotic manipulators, the *singular direction avoidance* (SDA) inverse steering law of Ford and Hall [17], inspired by e.g. Maciejewski and Klein [18], and the *generalized singularity-robust* (GSR) inverse [19] and subsequent improvement [20] by Wie *et al.*. Although the latter method constitutes the current state-of-the-art, for the given application there remain certain practical shortcomings that necessitate the design of a new control allocation scheme. Existing methods result in unnecessary tracking error, can become trapped in singular states, and are incapable of stabilizing the system once the gimbals have reached a "saturation" configuration, at which point tracking is no longer possible and sustained destabilizing oscillations are observed, all of which can have potentially harmful consequences to the human subject in our application.

We propose a new control scheme that strategically incorporates moment tracking errors to facilitate singularity escape or else stabilizes such singular configurations in which escape is not possible; to accomplish this, a novel approach to singularity taxonomy and proximity measurement is presented. With our control scheme, it is possible to safely realize a balancing device comparable to [3] for the case of $N = 2$ fixed-speed CMGs. This paper consists of a description of the CMG model in Section II, a discussion of singularities and their proposed measures in Section III, the proposition of a new control law in Section IV, and, finally, evaluation of the controller in simulations and physical testing in Sections V and VI.

II. System Model

A system composed of N CMGs can be modelled using Newton-Euler equations as by Schaub *et al.* [21], but with the distinction that the CMG subsystem dynamics are isolated from the structure to which they are attached, the human body. The net moment $\boldsymbol{M} \in \mathbb{R}^{3\times 1}$ applied to the CMG system (or, alternatively, the negative moment applied to the human) is:

$$\boldsymbol{M} = \mathbf{A}\dot{\boldsymbol{\gamma}} + \mathbf{B}\ddot{\boldsymbol{\gamma}} + \boldsymbol{d}\,, \tag{1}$$

where the control input is the vector of gimbal accelerations $\ddot{\boldsymbol{\gamma}} \in \mathbb{R}^{N\times 1}$, $\mathbf{A} \in \mathbb{R}^{3\times N}$ pertains to the gyroscopic moments (in the local $\hat{\boldsymbol{g}}_{t,i}$ directions as shown in Fig. 1), $\mathbf{B} \in \mathbb{R}^{3\times N}$ accounts for moments generated in the local $\hat{\boldsymbol{g}}_{g,i}$ directions due to acceleration of the gimbals, and $\boldsymbol{d} \in \mathbb{R}^{3\times 1}$ represents a component of the unintended *parasitic* gyroscopic moments induced via motion of the torso. These matrices are:

$$\begin{aligned}
\mathbf{A} &\coloneqq [\boldsymbol{a}_1, ..., \boldsymbol{a}_N] \\
\boldsymbol{a}_i &\coloneqq \hat{\boldsymbol{g}}_{s,i}(J_{T,s} - J_{T,t} + J_{T,g})\omega_{t,i} \\
&\quad + \hat{\boldsymbol{g}}_{t,i}[(J_{T,s} - J_{T,t} - J_{T,g})\omega_{s,i} + J_{W,s}\Omega_i] \\
\mathbf{B} &\coloneqq J_{T,g}[\hat{\boldsymbol{g}}_{g,1}, ..., \hat{\boldsymbol{g}}_{g,N}] \\
\boldsymbol{d} &\coloneqq J_{W,s}\sum_{i=1}^{N}\Omega_i(\hat{\boldsymbol{g}}_{t,i}\omega_{g,i} - \hat{\boldsymbol{g}}_{g,i}\omega_{t,i})\,,
\end{aligned} \tag{2}$$

where $J_{T,s}$, $J_{T,t}$, $J_{T,g}$ are the combined gimbal and flywheel moments of inertia about the $\hat{\boldsymbol{g}}_s$, $\hat{\boldsymbol{g}}_t$, and $\hat{\boldsymbol{g}}_g$ axes, and $J_{W,s}$ is the $\hat{\boldsymbol{g}}_s$-axis component of the flywheel only. The vector $\boldsymbol{\omega} \in \mathbb{R}^{3\times 1}$ denotes the angular velocity of the human torso, with gimbal-fixed components ω_s, ω_t, and ω_g. Finally, Ω is the rotor angular velocity. For this model, it is assumed that the human incorporates the device mass into their own

dynamics so all terms associated with the rigid-body motion of the assembly are neglected. As balancing requires moment generation in only the axial plane of the wearer, the gimbal axes are oriented parallel with the wearer's longitudinal axis such that the gyroscopic moment is most effectively used.

The gimbal motor torque of the i-th CMG, u_i, is [21]:

$$u_i = J_{T,g}(\hat{\boldsymbol{g}}_{g,i}^T\dot{\boldsymbol{\omega}} + \ddot{\gamma}_i) - (J_{T,s} - J_{T,t})\omega_{s,i}\omega_{t,i} - J_{W,s}\Omega_i\omega_{t,i}\,, \tag{3}$$

and the corresponding power is thus $p_i = \dot{\gamma}_i u_i$.

III. Singularity Measures

A. Classifications of singularities

Tracking performance may be disrupted if the range of possible output moments loses a degree of freedom, occurring whenever the moment-generating axes $\hat{\boldsymbol{g}}_{t,i}$ align such that the gyroscopic Jacobian $\mathbf{A}$ in (1) loses rank and becomes singular. The left null-space of $\mathbf{A}$, consisting of null-vectors $\boldsymbol{n}_l$ such that $\boldsymbol{n}_l^T\mathbf{A} = \mathbf{0}$, describes the space in $\mathbb{R}^3$ in which no moment can be generated. In the case of a system with parallel gimbal axes, the gyroscopic moment nominally spans the axial plane but encountering a singularity, in which $\hat{\boldsymbol{g}}_{t,i}$ align parallel or anti-parallel (parallel with opposite sense), reduces this to a single line of action; the projection of the set $\boldsymbol{n}_l$ onto the axial plane forms a line called the *singular direction*, $\hat{\boldsymbol{s}}$.

Singularities pose the greatest threat to moment tracking when $\hat{\boldsymbol{s}}$ is aligned with the parasitic-compensated reference moment, $\boldsymbol{\tau}_{\text{ref}} = \boldsymbol{M}_{\text{ref}} - \boldsymbol{d}$; even if the vectors are slightly misaligned, degradation of performance may be significant. Conversely, performance may remain relatively unaffected if $\hat{\boldsymbol{s}}$ is oriented normal to $\boldsymbol{\tau}_{\text{ref}}$. Hence we propose to explicitly consider the orientation of the singular direction with respect to the commanded output direction as a basis for categorizing singularities: cases in which $\hat{\boldsymbol{s}}$ is (anti-)parallel or nearly (anti-)parallel to $\boldsymbol{\tau}_{\text{ref}}$ we will henceforth refer to as *reference-aligned (RA) singularities* and the remaining singularities, in which $\hat{\boldsymbol{s}}$ is not significantly projected in the direction of $\boldsymbol{\tau}_{\text{ref}}$, as *unaligned singularities*. This categorization is not formally made in the related literature, yet is implied by the concept of singular directions and surfaces [22].

Any case in which all the rotor angular momentum vectors $\boldsymbol{h}_i$ are maximally projected in a given direction is an *external singularity*, lying on the outer boundary of the envelope of allowable net momentum states $\boldsymbol{H} = \sum_{i=1}^{N}\boldsymbol{h}_i(\gamma_i) \in \mathbb{R}^3$; the external singularity in which all $\boldsymbol{h}_i$ are maximally projected in the direction of the command moment will be defined here as the *RA saturation singularity*. All remaining singular configurations lie within the momentum envelope and are hence referred to as *internal singularities*. Of the 2^N reference-aligned singular configurations in our planar system, one is the RA saturation singularity (Fig. 2a), one is another external singularity defined here as the *RA anti-saturation singularity* (Fig. 2b), and the remaining $2^N{-}2$ are internal singularities (Fig. 2c and d), which, when relevant, may be further classified by the applicability of null-motion for singularity escape [22].

The relevance of this for control is that, due to the differential relationship between $\boldsymbol{h}_i$ and the generated moment, all $\boldsymbol{h}_i$ are ultimately driven towards $\boldsymbol{\tau}_{\text{ref}}$ (i.e. the RA saturation singularity). Under the influences of a moment-tracking control law, this is an impassable state and represents the fundamental limitation of the system to generate a moment in a given direction. The remaining $2^N{-}1$ RA singularities behave as unstable equilibria that instantaneously prohibit tracking, but can be perturbed to resume a trajectory towards the saturation singularity. In contrast, unaligned singularities do not behave as equilibria and can be escaped without perturbation.

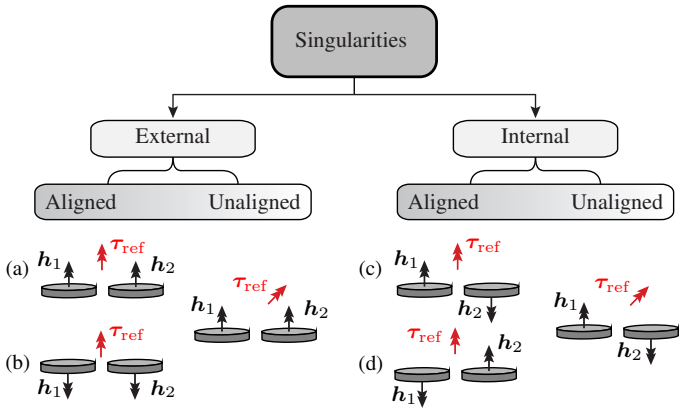

Fig. 2. Classifications of geometric singularities in a system of $N{=}2$ parallel fixed-speed single-gimbal CMGs, showing the relative orientations of the rotor angular momenta $\boldsymbol{h}_i$ and compensated reference moment $\boldsymbol{\tau}_{\text{ref}}$. Shown are all 2^N (reference-)aligned singularities and examples of the unaligned case.

B. Candidate singularity measures

To devise a singularity-robust control law, it is useful to define a measure of proximity to singular configurations. The most common selections are the manipulability measure [23] and square of the smallest singular value of $\mathbf{A}$, often associated with the SR and SDA gimbal steering laws, respectively. These values are computed respectively at each time instance k as:

$$\delta_{\text{SR}}(k) := \sqrt{\det\left(\mathbf{A}(k)\mathbf{A}^T(k)\right)}\,, \tag{4}$$

$$\delta_{\text{SDA}}(k) := \sigma_{\min}^2(\mathbf{A}(k))\,, \tag{5}$$

where each measure approaches zero as a singularity is encountered. A shortcoming of both is that they indicate only when a loss of freedom has occurred without regard to the direction of $\boldsymbol{\tau}_{\text{ref}}$, fundamentally consequential for tracking.

In their derivation of a feedback law, Oh and Vadali [24] defined an index that specifically considers the relationship of $\boldsymbol{\tau}_{\text{ref}}$ with the singular direction by computing the projection of $\boldsymbol{\tau}_{\text{ref}}$ onto the column space of $\mathbf{A}$. Adding a regularization value k_O, their *orthogonality index*, δ_O, can be expressed as:

$$\delta_O(k) := \frac{\boldsymbol{\tau}_{\text{ref}}^T(k)\mathbf{A}(k)\mathbf{A}^T(k)\boldsymbol{\tau}_{\text{ref}}(k)}{\boldsymbol{\tau}_{\text{ref}}^T(k)\boldsymbol{\tau}_{\text{ref}}(k) + k_O}\,, \tag{6}$$

which is zero when the requested moment is aligned with the singular direction and a maximum when it is spanned by $\mathbf{A}$.

The δ_{SR}, δ_{SDA}, and δ_{O} parameters are shown (normalized) in Fig. 3 for a system beginning in the anti-saturation singularity and ending in the saturation singularity, using a controller similar to [3]. For computing these parameters,

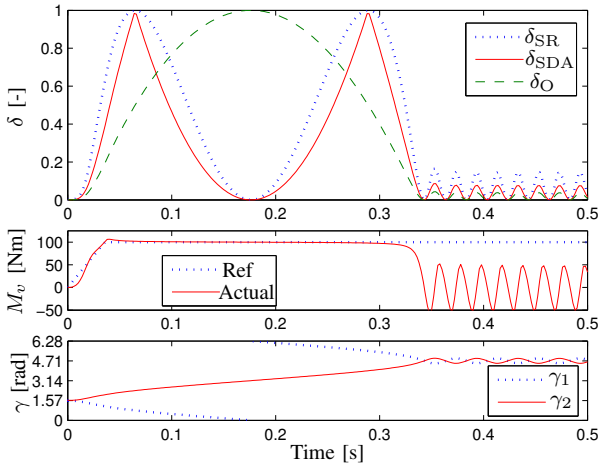

Fig. 3. Comparison of normalized singularity measures δ with plots of fall-axis output moment $\boldsymbol{M}_v$ and gimbal angles γ for a system starting near the singularity shown in Fig. 2b.

only the subspace of $\mathbf{A}$ that spans the axial plane of the wearer is used, since a parallel gimbal alignment entails that there will always be at least one dimension in which a net moment cannot be generated (in this case, the vertical axis). All three indices identify the initial singularity at t=0 s and the saturation singularity at $t\geq$0.33 s, but the SR and SDA measures identify an additional unaligned configuration at t=0.18 s, where the spin axes are anti-parallel (180° apart) but normal to the command moment direction – although a loss of freedom is incurred, no moment tracking error results. Thus, δ_O allows us to isolate the more problematic RA singularities.

Because the saturation singularity and remaining unsaturated external and internal singularities have distinct characteristics, we propose here separate singularity measures, δ_{sat} and δ_{uns}, respectively:

$$\delta_{\text{sat}}(k) \coloneqq 1 + p(\delta_O(k) - 1) \tag{7}$$

$$\delta_{\text{uns}}(k) \coloneqq 1 + (1-p)(\delta_O(k) - 1)\ , \tag{8}$$

where p is a binary scalar that is one when all projections $\boldsymbol{h}_i^T \boldsymbol{\tau}_{\text{ref}}$ are non-negative and zero otherwise.

IV. Control Design

A. Nominal controller

We first design a nominal controller that closely tracks the reference moment as long as no singularities are encountered. Because solving for $\ddot{\boldsymbol{\gamma}}$ directly in (1) results in undesirably high gimbal accelerations, a desired future reference gimbal velocity $\dot{\boldsymbol{\gamma}}_{\text{ref}}$ is instead specified and the acceleration is then chosen such that this reference is asymptotically tracked [24]:

$$\ddot{\boldsymbol{\gamma}} = k_{\dot{\gamma}}(\dot{\boldsymbol{\gamma}}_{\text{ref}} - \dot{\boldsymbol{\gamma}}) + \ddot{\boldsymbol{\gamma}}_{\text{ref}}\ , \tag{9}$$

where $k_{\dot{\gamma}}$ is a positive scalar gain and $\ddot{\boldsymbol{\gamma}}_{\text{ref}}$ is assumed small and is neglected. Substituting this into (1) yields:

$$\boldsymbol{M} = \mathbf{A}\dot{\boldsymbol{\gamma}}_{\text{ref}} + \mathbf{B}k_{\dot{\gamma}}(\dot{\boldsymbol{\gamma}}_{\text{ref}} - \dot{\boldsymbol{\gamma}}) + \boldsymbol{d}\ , \tag{10}$$

where $\dot{\boldsymbol{\gamma}}$ is the current (measured) gimbal velocity. To respect actuator limitations and minimize power consumption, we compute the reference gimbal rates as the minimizing solution to a weighted cost function of moment tracking errors, gimbal motor torques, and gimbal motor powers at each instance [3]:

$$\begin{aligned} J(k) &= \boldsymbol{\epsilon}_M^T(k)\mathbf{W}_M\boldsymbol{\epsilon}_M(k) + \boldsymbol{u}^T(k)\mathbf{W}_u\boldsymbol{u}(k) \\ &\quad + \boldsymbol{p}^T(k)\mathbf{W}_p\boldsymbol{p}(k) \\ &= (\boldsymbol{f}(k) - \mathbf{E}(k)\dot{\boldsymbol{\gamma}}_{\text{ref}}(k))^T\mathbf{W}(\boldsymbol{f}(k) - \mathbf{E}(k)\dot{\boldsymbol{\gamma}}_{\text{ref}}(k))\ , \end{aligned} \tag{11}$$

where the tracking error is $\boldsymbol{\epsilon}_M = \boldsymbol{M}_{\text{ref}} - \boldsymbol{M}$ and the weighting matrices are expressed as $\mathbf{W}_M = w_M\mathbf{I}_{3\times3}$, $\mathbf{W}_u = w_u\mathbf{I}_{N\times N}$, and $\mathbf{W}_p = w_p\mathbf{I}_{N\times N}$, where w_M, w_u, and w_p are all scalar design parameters. Stacking all the terms together, the cost function can be expressed with the following matrices:

$$\begin{aligned} \mathbf{E}(k) &\coloneqq \begin{bmatrix} \mathbf{E}_M(k) \\ \mathbf{E}_u \\ \mathbf{E}_p(k) \end{bmatrix} & \boldsymbol{f}(k) &\coloneqq \begin{bmatrix} \boldsymbol{f}_M(k) \\ \boldsymbol{f}_u(k) \\ \boldsymbol{f}_p(k) \end{bmatrix} \\ &\in \mathbb{R}^{(3+2N)\times N} & &\in \mathbb{R}^{(3+2N)\times 1} \\ \mathbf{W} &\coloneqq \text{diag}\,(\mathbf{W}_M, \mathbf{W}_u, \mathbf{W}_p) \in \mathbb{R}^{(3+2N)\times(3+2N)}\ , \end{aligned} \tag{12}$$

where the moment-tracking part is:

$$\begin{aligned} \mathbf{E}_M &= \mathbf{A}(k) + \mathbf{B}(k)k_{\dot{\gamma}} \\ \boldsymbol{f}_M &= \boldsymbol{M}_{\text{ref}}(k) - \boldsymbol{d}(k) + \mathbf{B}(k)k_{\dot{\gamma}}\dot{\boldsymbol{\gamma}}(k)\ . \end{aligned} \tag{13}$$

Upon substitution of (9) into (3), the gimbal motor torques $\boldsymbol{u}$ can be expressed as $\boldsymbol{u} = \mathbf{E}_u\dot{\boldsymbol{\gamma}}_{\text{ref}} - \boldsymbol{f}_u$, where:

$$\begin{aligned} \mathbf{E}_u &\coloneqq J_{T,g}k_{\dot{\gamma}}\mathbf{I}_{N\times N} \\ \boldsymbol{f}_u &\coloneqq [f_{u,1}, ..., f_{u,N}]^T \\ f_{u,i} &\coloneqq J_{T,g}(k_{\dot{\gamma}}\dot{\gamma}_i - \hat{\boldsymbol{g}}_{g,i}^T\dot{\boldsymbol{\omega}}) \\ &\quad + [(J_{T,s} - J_{T,t})\omega_{s,i} + J_{W,s}\Omega_i]\omega_{t,i}\ . \end{aligned} \tag{14}$$

Because the gimbal motor powers are quadratic in $\dot{\boldsymbol{\gamma}}_{\text{ref}}$, a first-order Taylor series expansion of $\dot{\boldsymbol{\gamma}}_{\text{ref}}^{\circ 2}$ is made about the measured rate $\dot{\boldsymbol{\gamma}}$, where $\circ$ is the element-wise product:

$$\begin{aligned} \dot{\boldsymbol{\gamma}}_{\text{ref}}^{\circ 2} &= \dot{\boldsymbol{\gamma}}^{\circ 2} + 2\dot{\boldsymbol{\gamma}} \circ (\dot{\boldsymbol{\gamma}}_{\text{ref}} - \dot{\boldsymbol{\gamma}}) + O(\dot{\boldsymbol{\gamma}}_{\text{ref}}^{\circ 2}) \\ &\approx 2\dot{\boldsymbol{\gamma}} \circ \dot{\boldsymbol{\gamma}}_{\text{ref}} - \dot{\boldsymbol{\gamma}}^{\circ 2}\ . \end{aligned} \tag{15}$$

The future gimbal motor powers can then be expressed as:

$$\begin{aligned} \boldsymbol{p} &= \dot{\boldsymbol{\gamma}}_{\text{ref}} \circ \boldsymbol{u} \\ &= \mathbf{E}_u\dot{\boldsymbol{\gamma}}_{\text{ref}}^{\circ 2} - \boldsymbol{f}_u \circ \dot{\boldsymbol{\gamma}}_{\text{ref}} \\ &\approx \mathbf{E}_p\dot{\boldsymbol{\gamma}}_{\text{ref}} - \boldsymbol{f}_p\ , \end{aligned} \tag{16}$$

where:

$$\begin{aligned} \mathbf{E}_p &\coloneqq 2\mathbf{E}_u\text{diag}(\dot{\boldsymbol{\gamma}}) - \text{diag}(\boldsymbol{f}_u) \\ \boldsymbol{f}_p &\coloneqq \mathbf{E}_u\dot{\boldsymbol{\gamma}}^{\circ 2}\ . \end{aligned} \tag{17}$$

The minimizing solution to (11) at each sample instance is then computed as the weighted Moore-Penrose pseudoinverse:

$$\begin{aligned} \dot{\boldsymbol{\gamma}}_{\text{ref}}(k) &= \left(\mathbf{E}^T(k)\mathbf{W}(k)\mathbf{E}(k)\right)^{-1}\mathbf{E}^T(k)\mathbf{W}(k)\boldsymbol{f}(k) \\ &= \mathbf{E}_{\text{W}}^{+}(k)\boldsymbol{f}(k)\ . \end{aligned} \tag{18}$$

Although tuning of the weights can limit the motor torques and powers to within an acceptable range, adding hard inequality constraints ensures optimality even in the presence of motor saturation. For bounds on both the allowable torque and power,

there are a total of $4N$ inequality constraints; because not all can be active at the same time, it is necessary to check the Karush-Kuhn-Tucker conditions at only 3^N combinations of equality constraints. Posing each combination as $\mathbf{G}\dot{\boldsymbol{\gamma}} = \boldsymbol{h}$ such that $\mathbf{G}$ has linearly independent rows, the constrained solution $\overline{\dot{\boldsymbol{\gamma}}}_{\text{ref}}$ can be expressed as a function of $\dot{\boldsymbol{\gamma}}_{\text{ref}}$ from (18):

$$\begin{aligned}\overline{\dot{\boldsymbol{\gamma}}}_{\text{ref}} &= \dot{\boldsymbol{\gamma}}_{\text{ref}} \\ &- (\mathbf{E}^T\mathbf{W}\mathbf{E})^{-1}\mathbf{G}^T\left[\mathbf{G}(\mathbf{E}^T\mathbf{W}\mathbf{E})^{-1}\mathbf{G}^T\right]^{-1}(\mathbf{G}\dot{\boldsymbol{\gamma}}_{\text{ref}} - \boldsymbol{h})\,.\end{aligned} \tag{19}$$

B. Singularity robustness

Although the motor torque and power penalties prevent $\mathbf{E}$ from becoming numerically singular, hence maintaining a finite $\dot{\boldsymbol{\gamma}}_{\text{ref}}$ and performing a function similar to SR-type methods, performance remains poor near aligned geometric singularities – in particular, gimbal overshooting and oscillation occur at the saturation singularity, resulting in a fluctuating output moment (Fig. 3, $t{\geq}0.33\,\text{s}$), and the controller cannot resolve indeterminism at the other aligned singularities, leaving the gimbals in a locked state. There has been little mention of the former issue in the related literature since, in aerospace applications, the gimbal rates are relatively small and the reference moment profile is adjusted to avoid the approach of such configurations either by pre-manoeuvre momentum management schemes or in real-time using thrusters [25]. Although the indeterminism problem can in some cases be solved by gradient-free null-motion algorithms, requiring redundancy, the perturbation injection method of Wie *et al.* [19] is applicable to all types of unstable singularities and any number of actuators. The crucial feature of this method, adapted to our framework, is the modulation of the off-diagonal elements of $\mathbf{W}_M$ to produce an error in the direction of the output moment and perturb the gimbal states, after which the nominal controller can function without issue. Using a modulation function $\epsilon_i = \epsilon_0 \sin(\omega_\epsilon t + \phi_i)$, where ϵ_0, ω_ϵ, and ϕ_i and are all scalar design parameters, $\mathbf{W}_M$ can be expressed as [19]:

$$\mathbf{W}_M(k) = w_M \begin{bmatrix} 1 & \epsilon_3 & \epsilon_2 \\ \epsilon_3 & 1 & \epsilon_1 \\ \epsilon_2 & \epsilon_1 & 1 \end{bmatrix}^{-1} . \tag{20}$$

Although this method is very effective when the objective is only moment tracking, when combined with other performance criteria, such as minimal motor torque and power, such an indirect approach can result in significant delay in escaping singularities. Thus, to overcome performance issues at aligned singularities, new control techniques are required.

Since moment tracking can no longer be reliably sustained when approaching the saturation configuration, one solution is to dynamically change the cost function penalties such that tracking is abandoned in favour of stability. To achieve this, a penalty $\mathbf{W}_{\text{sat}} = w_{\text{sat}}\mathbf{I}_{N\times N}$ on the gimbal rates $\dot{\boldsymbol{\gamma}}_{\text{ref}}$ is proposed, such that gimbal damping is increased with proximity to saturation and the output moment is gradually arrested:

$$w_{\text{sat}}(k) = k_{\text{sat},1}\delta_{\text{sat}}^{-k_{\text{sat},2}}(k)\,, \tag{21}$$

where $k_{\text{sat},1}, k_{\text{sat},2} > 0$ are both scalar design variables and δ_{sat} is the measure of proximity to the saturation singularity as defined in (7). If the command moment direction changes, the magnitude of damping declines and the gimbals are no longer restricted in their motions. The parameters $k_{\text{sat},1}$ and $k_{\text{sat},2}$ are tuned such that the damping grows large enough to prevent oscillations and abrupt enough to avoid impacting performance away from saturation.

In order to escape from an unstable unsaturated aligned singularity, the system states must be perturbed in some manner, which can be as simple as adding noise to the state measurement, or it can be in the form of a deliberate deterministic perturbation, as in (20). A more direct approach is to exploit the symmetry of the system in question and force the gimbals apart in predetermined directions. To do this, the reference gimbal velocities can be computed as if each gimbal is perturbed by some angle $\Delta\gamma_i > 0$ from singularity – for example, by neglecting $\mathbf{B}$ from (10) and ignoring the parasitic moment terms in the $\mathbf{A}$ matrix, the i-th gimbal rate near the unsaturated singularity can be computed approximately as:

$$\dot{\gamma}_{\text{uns},i}(k) = \alpha_i \frac{||\boldsymbol{\tau}_{\text{ref}}(k)||_2}{NJ_{W,s}\Omega_i(k)\sin(\Delta\gamma_i)}\,, \tag{22}$$

where, for simplicity, it is assumed that each CMG equally contributes to the output moment. The perturbation from singularity can be selected as an arbitrary small nonzero angle, such as $\Delta\gamma_i = 5^\circ$, for instance. The variable $\alpha_i = \{-1, 0, 1\}$ determines the desired direction of rotation of each gimbal, based on some pre-defined criteria; for a system of two CMGs, a logical choice would be $[\alpha_1, \alpha_2] = [-1, 1]$ such that the gimbals are driven in opposite directions. Because such a perturbation would, in reality, be only very local and accurate modelling is not necessary, an alternative would be to amalgamate the expression into a single scalar unsaturated-singularity-escape design parameter $k_{\text{uns},\tau}$:

$$\dot{\gamma}_{\text{uns},i}(k) = \alpha_i k_{\text{uns},\tau}\,||\boldsymbol{\tau}_{\text{ref}}(k)||_2\,. \tag{23}$$

To disengage the evasive action once the states have been sufficiently perturbed, the associated weighting should decrease with increasing singularity measure δ_{uns} and gimbal inertia:

$$\mathbf{W}_{\text{uns}}(k) = \mathrm{e}^{-(k_{\text{uns},\delta}\delta_{\text{uns}}(k) + k_{\text{uns},\dot{\gamma}}\dot{\boldsymbol{\gamma}}^T(k)\dot{\boldsymbol{\gamma}}(k))}\mathbf{I}_{N\times N}\,, \tag{24}$$

where $k_{\text{uns},\delta}$ and $k_{\text{uns},\dot{\gamma}}$ are additional non-negative scalar design variables that determine the sensitivity to singularity proximity and gimbal inertia, respectively.

Amending (12), the system becomes:

$$\begin{aligned}\overline{\mathbf{E}}(k) &\coloneqq \begin{bmatrix}\mathbf{E}(k)\\ \mathbf{I}_{N\times N}\\ \mathbf{I}_{N\times N}\end{bmatrix} \in \mathbb{R}^{(3+4N)\times N} \qquad \overline{\boldsymbol{f}}(k) \coloneqq \begin{bmatrix}\boldsymbol{f}\\ \mathbf{0}_{N\times 1}\\ \dot{\boldsymbol{\gamma}}_{\text{uns}}(k)\end{bmatrix} \in \mathbb{R}^{(3+4N)\times 1} \\ \overline{\mathbf{W}}(k) &\coloneqq \text{diag}\big(\mathbf{W}, \mathbf{W}_{\text{sat}}(k), \mathbf{W}_{\text{uns}}(k)\big) \in \mathbb{R}^{(3+4N)\times(3+4N)}\,,\end{aligned} \tag{25}$$

which can be solved as in (18). To avoid computing an infinite damping penalty as in (21), we can define its analytic inverse as $w_{\text{sat}}^{\#} = k_{\text{sat},1}^{-1}\delta_{\text{sat}}^{k_{\text{sat},2}}$ and reformulate (18) to the following:

$$\dot{\boldsymbol{\gamma}}_{\text{ref}} = \mathbf{E}^*\boldsymbol{f} + \boldsymbol{\beta}^*\dot{\boldsymbol{\gamma}}_{\text{uns}} \tag{26}$$

where:

$$\begin{aligned} \mathbf{E}^* &= \mathbf{\Lambda}\mathbf{E}^T\mathbf{W}\ , \qquad\qquad \boldsymbol{\beta}^* = \mathbf{\Lambda}\mathbf{W}_{\text{uns}} \\ \mathbf{\Lambda} &= w_{\text{sat}}^{\#}\left(w_{\text{sat}}^{\#}(\mathbf{E}^T\mathbf{W}\mathbf{E} + \mathbf{W}_{\text{uns}}) + \mathbf{I}_{N\times N}\right)^{-1}\ . \end{aligned} \tag{27}$$

Replacing $(\mathbf{E}^T\mathbf{W}\mathbf{E})^{-1}$ with $\mathbf{\Lambda}$, (19) can again be used to account for motor constraints.

Because different singularity handling techniques are used depending on the gimbal orientations with respect to the reference moment direction, we name this the *directional singularity-robust* (DSR) control allocation law.

C. Stability analysis

Regardless of whether the current objective is moment tracking or stabilization of the gimbals at the saturation singularity (or some intermediate combination of the two), we can pose the problem as one of tracking a desired gimbal rate $\dot{\boldsymbol{\gamma}}_{\text{ref}}$. First we consider a constant or slowly-varying $\boldsymbol{M}_{\text{ref}}$. Selecting the following Lyapunov function [24]:

$$V(\dot{\boldsymbol{\gamma}}) = \frac{1}{2}(\dot{\boldsymbol{\gamma}}_{\text{ref}} - \dot{\boldsymbol{\gamma}})^T(\dot{\boldsymbol{\gamma}}_{\text{ref}} - \dot{\boldsymbol{\gamma}})\ , \tag{28}$$

differentiating with respect to time, taking $\ddot{\boldsymbol{\gamma}}_{\text{ref}} \approx 0$, and substituting (9) for $\ddot{\boldsymbol{\gamma}}$ yields:

$$\begin{aligned} \dot{V}(\dot{\boldsymbol{\gamma}}) &= (\dot{\boldsymbol{\gamma}}_{\text{ref}} - \dot{\boldsymbol{\gamma}})^T(\ddot{\boldsymbol{\gamma}}_{\text{ref}} - \ddot{\boldsymbol{\gamma}}) \\ &= -k_{\dot{\gamma}}(\dot{\boldsymbol{\gamma}}_{\text{ref}} - \dot{\boldsymbol{\gamma}})^T(\dot{\boldsymbol{\gamma}}_{\text{ref}} - \dot{\boldsymbol{\gamma}})\ . \end{aligned} \tag{29}$$

Thus, asymptotic tracking of the reference gimbal rate is guaranteed for any $k_{\dot{\gamma}} > 0$ and any $\dot{\boldsymbol{\gamma}}_{\text{ref}}$ that does not result in sustained motor saturation. Away from the saturation singularity and in the absence of modelling errors, $\dot{\boldsymbol{\gamma}}$ converging to $\dot{\boldsymbol{\gamma}}_{\text{ref}}$ together with (10) implies that $\boldsymbol{M}$ converges to $\boldsymbol{M}_{\text{ref}}$. As the saturation singularity $\boldsymbol{\gamma}_{\text{sat}}$ is approached, a transition to damping of the gimbals occurs once $\sigma_{\max}(\mathbf{E}) < (w_M w_{\text{sat}}^{\#})^{-\frac{1}{2}}$, where $\sigma_{\max}$ denotes the maximum singular value; by designing $w_{\text{sat}}^{\#}$ such that it decays to zero at $\boldsymbol{\gamma}_{\text{sat}}$, then $\mathbf{\Lambda}$ and $\dot{\boldsymbol{\gamma}}_{\text{ref}}$ will correspondingly decline to zero and the gimbals will come to rest. Although such issues were not encountered during our simulations or experimentation, it cannot be guaranteed that the gimbals will remain within this high damping region in the presence of significant motor saturation or poor tracking of $\dot{\boldsymbol{\gamma}}_{\text{ref}}$. If this issue cannot be solved via tuning, it is also possible to design a $w_{\text{sat}}^{\#}$ that remains zero in some continuous neighbourhood of $\boldsymbol{\gamma}_{\text{sat}}$ such that an equilibrium manifold exists, or else implement a supervisor that blocks subsequent mode switching.

To investigate the behaviour under arbitrary dynamic reference moments $\boldsymbol{M}_{\text{ref}}$, we can analyze stability in terms of passivity with respect to $\boldsymbol{M}_{\text{ref}}$ by finding a positive semidefinite storage function $S(\boldsymbol{x})$ that shows that the rate of energy accumulation is less than that supplied, closely linked to $\mathcal{L}_2$ stability. We select the kinetic energy of all flywheel-gimbal assemblies as our storage function candidate, where $\boldsymbol{\omega} = 0$ for simplicity and $\boldsymbol{x}^T = [\boldsymbol{\gamma}^T, \dot{\boldsymbol{\gamma}}^T]$:

$$S(\boldsymbol{x}) = \frac{1}{2}\left(J_{T,g}\dot{\boldsymbol{\gamma}}^T\dot{\boldsymbol{\gamma}} + J_{W,s}\mathbf{\Omega}^T\mathbf{\Omega}\right)\ . \tag{30}$$

Inserting $\dot{\mathbf{\Omega}} = \mathbf{0}$ and using (9), this has the time derivative:

$$\begin{aligned} \dot{S}(\boldsymbol{x}) &= J_{T,g}\dot{\boldsymbol{\gamma}}^T\ddot{\boldsymbol{\gamma}} \\ &= J_{T,g}k_{\dot{\gamma}}\dot{\boldsymbol{\gamma}}^T(\dot{\boldsymbol{\gamma}}_{\text{ref}} - \dot{\boldsymbol{\gamma}})\ . \end{aligned} \tag{31}$$

For convenience, we also define $\boldsymbol{f}_{\text{ref}} = \mathbf{E}\dot{\boldsymbol{\gamma}}_{\text{nom}}$, with $\dot{\boldsymbol{\gamma}}_{\text{nom}}$ a virtual reference gimbal rate that results in close moment tracking (exact if $w_u, w_p = 0$), yet grows excessively near singularities. We then obtain:

$$\begin{aligned} \dot{S}(\boldsymbol{x}) &= J_{T,g}k_{\dot{\gamma}}\left(\dot{\boldsymbol{\gamma}}^T\mathbf{E}^*\mathbf{E}\dot{\boldsymbol{\gamma}}_{\text{nom}} + \dot{\boldsymbol{\gamma}}^T\boldsymbol{\beta}^*\dot{\boldsymbol{\gamma}}_{\text{uns}} - \dot{\boldsymbol{\gamma}}^T\dot{\boldsymbol{\gamma}}\right) \\ &\leq J_{T,g}k_{\dot{\gamma}}\left(\dot{\boldsymbol{\gamma}}^T\dot{\boldsymbol{\gamma}}_{\text{nom}} + \dot{\boldsymbol{\gamma}}^T\dot{\boldsymbol{\gamma}}_{\text{uns}}\right)\ . \end{aligned} \tag{32}$$

where the bottom line is the (transformed) supply rate and both $\text{eig}(\mathbf{E}^*\mathbf{E})_i, \text{eig}(\boldsymbol{\beta}^*)_i \in [0, 1]$ go to zero $\forall i \in [1, N]\cap\mathbb{Z}$ as $\boldsymbol{\gamma}_{\text{sat}}$ is approached and $w_{\text{sat}}^{\#} \to 0$. Thus, we can guarantee that the system never stores more energy than would be injected by tracking the reference. As the saturation singularity is approached, the rate of energy accumulation decays, while the final term of the top line ensures that energy is dissipated to bring the gimbals to rest. Finally, we also see the role that $\dot{\boldsymbol{\gamma}}_{\text{uns}}$ plays to inject energy into the system to escape unsaturated aligned singularities.

V. Controller evaluation

A. Simulation study

The focus of this assessment is on the singularity handling of the DSR controller in (25) in relation to the static-weight (SW) controller in (12), rather than the nominal tracking performance. It is assumed that the person falls rigidly with a fixed point of rotation about one foot and can be modelled as an inverted pendulum with three degrees of rotational freedom and moment of inertia $\mathbf{J}_H = \text{diag}(J_{H,u}, J_{H,v}, J_{H,w})$ as in [3], where u, v, and w pertain to the directions of the wearer's anterior, left, and longitudinal axes, respectively (Fig. 4a). The attitude of the human is expressed in Euler 3-2-3 rotations as denoted by $[\theta_1, \theta_2, \theta_3]$. The person is assumed to be initially leaning forward by θ_2=5° when a loss of balance is detected, followed by a free fall from rest. The gimbals begin in the anti-saturation singularity shown in Fig. 2b. The moment profile begins with a ramp of 2800 Nm/s and is sustained at the maximum value of 100 Nm such that the system eventually encounters the saturation singularity. It is assumed that all states can be measured accurately and detection of loss of balance is reliably performed. The controller was simulated at 500 Hz and the human states were integrated using the MATLAB function `ode45` to approximate continuous time. All model and control parameters are listed in Table I.

Because the SW controller would otherwise have no ability to escape the initial unstable singularity, the method of Wie *et al.* was incorporated by using the moment-tracking penalty matrix in (20) with w_M=100 Nm^{-1}, ω_ϵ=100 Hz, and $\phi_i = i \cdot 2\pi/3$ rad. To eliminate unnecessary tracking error away from singularity, ϵ_0 was scaled with δ_{uns} as $\epsilon_0 = \text{e}^{-10^4\delta_{\text{uns}}}$.

B. Experimental study

A similar test was performed with a single CMG mounted to an inverted pendulum with one rotational degree of freedom

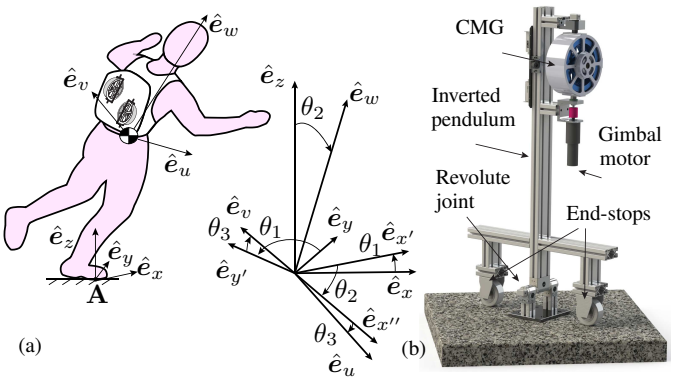

Fig. 4. (a) Schematic showing mapping from inertially-fixed frame $\mathcal{N}$: $\{\hat{\boldsymbol{e}}_x, \hat{\boldsymbol{e}}_y, \hat{\boldsymbol{e}}_z\}$ to body-fixed coordinates $\mathcal{B}$: $\{\hat{\boldsymbol{e}}_u, \hat{\boldsymbol{e}}_v, \hat{\boldsymbol{e}}_w\}$ using Euler 3-2-3 coordinates. (b) Test apparatus consisting of a single CMG on a single-degree-of-freedom inverted pendulum.

TABLE I
SIMULATION (SIM) AND EXPERIMENT (EXP) PARAMETERS.

Parameter	Value (sim)	Value (exp)	Units
N	2	1	-
Ω	1650	419	rad/s
$\boldsymbol{\theta}(t_0)$	$[0, 5, 0]$	-	deg
$\boldsymbol{\omega}(t_0)$	$[0, 0, 0]$	-	rad/s
$J_{W,s}$	$3.60 \cdot 10^{-3}$	$2.00 \cdot 10^{-2}$	kgm^2
$J_{T,s}$	$3.60 \cdot 10^{-3}$	$4.00 \cdot 10^{-2}$	kgm^2
$J_{T,t}$	$1.80 \cdot 10^{-3}$	$2.24 \cdot 10^{-2}$	kgm^2
$J_{T,g}$	$1.8 \cdot 10^{-3}$	$3.97 \cdot 10^{-2}$	kgm^2
$u_{\max}$	10	10	Nm
$p_{\max}$	80	150	W
$J_{H,u} = J_{H,v}$	69.0	-	kgm^2
$J_{H,w}$	3.15	-	kgm^2
m_H	70	-	kg
h_H	0.85	-	m
$k_{\dot{\gamma}}$	500	378	s^{-1}
w_M	100	100	Nm^{-1}
w_u	10	10	Nm^{-1}
w_p	1	1	W^{-1}
$k_{\text{sat},1}$	1	1	s/rad
$k_{\text{sat},2}$	2	2	-
$[\alpha_1, \alpha_2]$	$[-1, 1]$	1	-
$k_{\text{uns},\tau}$	5	5	s/rad
$k_{\text{uns},\delta}$	10^4	10^4	-
$k_{\text{uns},\dot{\gamma}}$	0	0	(s/rad)^2

as described in [26] (Fig. 4b). Due to the diminished degrees of freedom, only the moment projected along a single axis is tracked. The moment profile is the same as in simulations, but with the ramp rate and maximum value decreased by a factor of ten. Friction and gear backlash are neglected in the modelling and, because of the current lack of motor current sensors and force sensors, the motor efforts and output moment are estimated from the system states and the model.

Because (20) is not applicable for tracking in a single dimension, separate tests were performed for comparing unsaturated and saturated singularity handling – the former with the gimbals oriented $\gamma(0)=\pi$ rad from the external singularity, and the latter with $\gamma(0)=\pi/2$ rad. For safety, the pendulum was constrained in the vertical position. As in the simulations, the sampling frequency is 500 Hz. The experiment parameters and measured apparatus properties are shown in Table I.

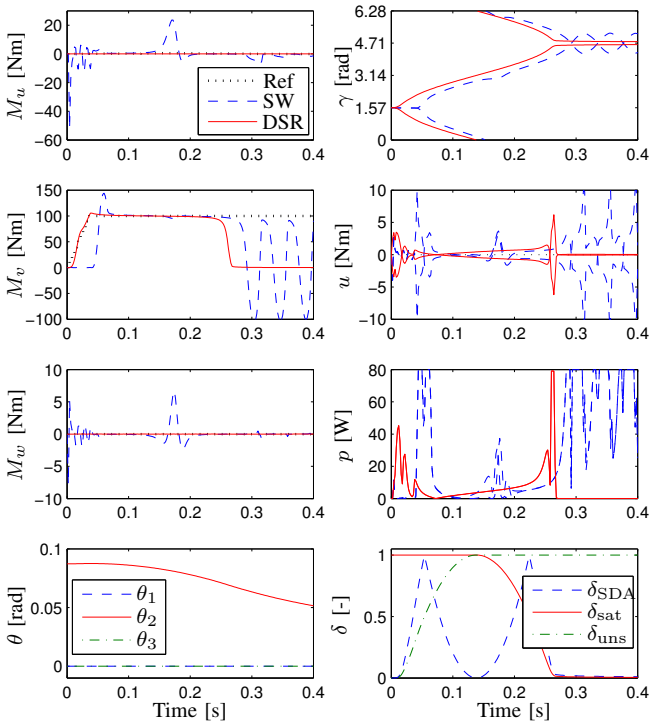

Fig. 5. Simulation results for the SW and DSR controllers for gimbals initially at the anti-saturation singularity. Shown are the moments projected onto the human-fixed axes (M_u, M_v, M_w), the human attitude (θ), the gimbal angles (γ), the gimbal motor torques (u), the gimbal motor powers (p), and singularity measures (δ).

C. Results

The simulation results in Fig. 5 reveal that the proposed unstable singularity escape procedure results in approximately 80% shorter delay, and, consequently, does not incur the same tracking errors as the method of Wie *et al.* for this system; furthermore, the oscillations imposed by the latter method prior to escape are noticeable and may result in either discomfort or destabilization of the subject. It is also observed that gimbal overshooting at the external singularity (∼0.3 s) is successfully avoided by the the damping action of the proposed DSR scheme, contributing to greater stability of the controller.

The experimental results in Fig. 6, beginning from the anti-saturation singularity, show that the DSR singularity escape procedure is successful, but poor tracking of the gimbal rates due to unmodelled power supply dynamics results in visible oscillations; conversely, the system without escape functionality remains locked, despite the presence of sensor noise. Beginning instead at $\pi/2$ rad from the saturation singularity (Fig. 7), it is again observed that the DSR law successfully damps the gimbal swinging at 1 s.

VI. Discussion

Both simulation and experiment results indicate that, for the present application, the proposed DSR controller effectively reduces tracking performance degradation at all aligned

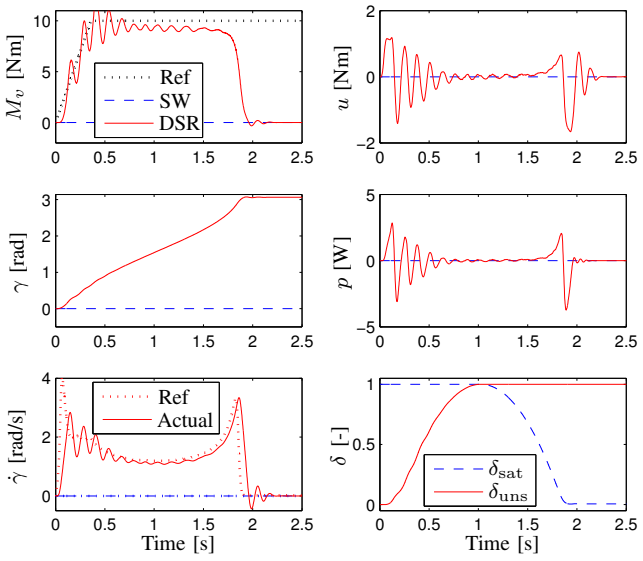

Fig. 6. Experimental results for the SW and DSR controllers for the spin axis initially π rad from the external singularity. Shown are the moment projected in the command direction (M_v), the gimbal angular displacement (γ), reference and actual gimbal rates ($\dot{\gamma}$), approximate gimbal motor torque (u) and power (p), and singularity proximity measures (δ).

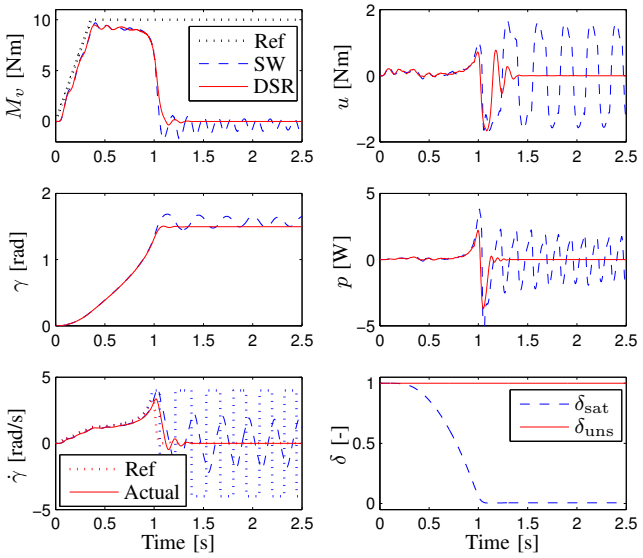

Fig. 7. Experimental results for the SW and DSR controllers for the spin axis initially $\pi/2$ rad from the external singularity. Shown are the moment projected in the command direction (M_v), the gimbal angular displacement (γ), reference and actual gimbal rates ($\dot{\gamma}$), approximate gimbal motor torque (u) and power (p), and singularity proximity measures (δ).

singularities while not significantly altering the nominal performance. For the proposed application, this signifies great progress towards the safe use of CMGs as wearable actuators. These results suggest it is possible to sustain a 100 Nm output for up to 0.25 s using a device projected to weigh less than 3 kg and consume on average 16 W of power when the gimbals are active or 5 J per manoeuvre (not accounting for losses or the power required to maintain flywheel speed). Further work in this study must be directed towards designing a control scheme that is passive with respect to $\boldsymbol{\omega}$ to ensure the safety of the wearer under any scenario.

Although specifically designed for a non-redundant system, these control techniques may still be applicable to impassable singularities in redundant systems in which null-motion is ineffective. This controller may also be relevant for a growing number of terrestrial balancing applications such as unstable vehicles including scooters (e.g. C-1 electric scooter, Lit Motors, USA), bicycles [27], unicycles [28], other personal transportation devices (e.g. the EMBRIO, Bombardier, Canada, and the eniCycle, eniCycle, Slovenia), single-wheel robots [29], and underwater vehicles [30], in addition to micro satellites and space manipulators [31], [32].

VII. Conclusion

By adding cost function penalties that scale with proximity to the relevant classes of singularities, we demonstrated that, with the proposed *directional singularity robust* (DSR) control law, adverse moment tracking behaviour of CMGs near internal and external singularities can be reliably mitigated, thereby improving the ability of a wearable CMG assembly to successfully stabilize an unbalanced subject. We showed that our method escapes unstable singularities up to 80% faster than the state-of-the-art, while successfully damping oscillations at the saturation configuration.

Acknowledgment

This research was supported by the U.S. Department of Education, National Institute on Disability and Rehabilitation Research, NIDRR-RERC, Grant Number H133E120010, and by the Marie-Curie career integration grant PCIG13-GA-2013-618899. The authors would also like to thank Jan van Frankenhuyzen, Guus Liqui Lung, and Simon Toet for technical support.

References

[1] M. Muehlebach, G. Mohanarajah, and R. D'Andrea, "Nonlinear analysis and control of a reaction wheel-based 3D inverted pendulum," in *Conference on Decision and Control*, Florence, Italy, 2013.

[2] T. Wojtara, M. Sasaki, H. Konosu, M. Yamashita, S. Shimoda, F. Alnajjar, and H. Kimura, "Artificial balancer – supporting device for postural reflex," *Gait & Posture*, vol. 35, pp. 316–321, 2012.

[3] D. Li and H. Vallery, "Gyroscopic asistance for human balance," in *12th IEEE International Workshop on Advanced Motion Control (AMC)*, Sarajaevo, Bosnia and Herzegovina, March 25-27 2012.

[4] R. Matsuzaki and Y. Fujimoto, "Walking assist device using control moment gyroscopes," in *IEEE Industrial Electronics Society Annual Conference (IECON)*, Vienna, November 10-13 2013.

[5] J. Chiu and A. Goswami, "Design of a wearable scissored-pair control moment gyroscope (SP-CMG) for human balance assist," in *ASME International Design Engineering Technical Conferences & Computers and Information in Engineering Conference (IDET/CIE)*, Buffalo, August 17-20 2014.

[6] H. Kurokawa, "Survey of theory and steering laws of single-gimbal control moment gyros," *Journal of Guidance, Control, and Dynamics*, vol. 30, no. 5, pp. 1331–1340, 2007.

[7] H. Vallery, A. Bögel, C. O'Brien, and R. Riener, "Cooperative control design for robot-assisted balance during gait," *Automatisierungstechnik*

Methoden und Anwendungen der Steuerungs-, Regelungs- und Informationstechnik, vol. 60, no. 11, pp. 715–720, 2012.

[8] S. R. Vadali, H.-S. Oh, and S. R. Walker, "Preferred gimbal angles for single gimbal control moment gyros," *Journal of Guidance, Control, and Dynamics*, vol. 13, no. 6, pp. 1090–1095, 1990.

[9] O. Tekinalp and E. Yavuzoğlu, "A new steering law for redundant control moment gyroscope clusters," *Aerospace Science and Technology*, vol. 9, no. 7, pp. 626–634, October 2005.

[10] J. A. Paradiso, "Global steering of single gimballed control moment gyroscopes using a directed search," *Journal of Guidance, Control, and Dynamics*, vol. 15, no. 5, pp. 1236–1244, 1992.

[11] K. Takada and H. Kojima, "Receding horizon control on steering of control moment gyro for fast attitude maneuver," *Transactions of the Japanese Society for Aeronautical and Space Sciences*, vol. 52, no. 175, pp. 1–10, 2009.

[12] Y. Ikeda, T. Nakajima, and Y. Chida, "Attitude control of spacecraft by NMPC with consideration of singularity avoidance of CMG," in *51st IEEE Conference on Decision and Control*, Maui, Hawaii, USA, December 10-13 2012.

[13] D. E. Cornick, "Singularity avoidance control laws for single gimbal control moment gyros," *American Institute of Aeronautics and Astronautics paper # 79-1698*, pp. 20–33, August 1979.

[14] N. S. Bedrossian, J. Paradiso, E. V. Bergmann, and D. Rowell, "Steering law design for redundant single-gimbal control moment gyroscopes," *Journal of Guidance, Control, and Dynamics*, vol. 13, no. 6, pp. 1083–1089, 1990.

[15] C. W. Wampler, "Manipulator inverse kinematic solutions based on vector formulations and damped least-squares methods," *IEEE Transactions on Systems, Man, and Cybernetics*, vol. 16, no. 1, pp. 93–101, January/February 1986.

[16] Y. Nakamura and H. Hanafusa, "Inverse kinematic solutions with singularity robustness for robot manipulator control," *Journal of Dynamic Systems, Measurement, and Control*, vol. 108, pp. 163–171, September 1986.

[17] K. A. Ford and C. D. Hall, "Singular direction avoidance steering for control-moment gyros," *Journal of Guidance, Control, and Dynamics*, vol. 23, no. 4, pp. 648–656, July-August 2000.

[18] A. A. Maciejewski and C. A. Klein, "Numerical filtering for the operation of robotic manipulators through kinematically singular configurations," *Journal of Robotic Systems*, vol. 5, no. 6, pp. 527–552, 1988.

[19] B. Wie, D. Bailey, and C. Heiberg, "Singularity robust steering logic for redundant single-gimbal control moment gyros," *Journal of Guidance, Control, and Dynamics*, vol. 24, no. 5, pp. 865–872, September-October 2001.

[20] B. Wie, "Singularity escape/avoidance steering logic for control moment gyro systems," *Journal of Guidance, Control, and Dynamics*, vol. 28, no. 5, pp. 948–956, September-October 2005.

[21] H. Schaub, S. R. Vadali, and J. L. Junkins, "Feedback control law for variable speed control moment gyros," *Journal of the Astronautical Sciences*, vol. 46, no. 3, pp. 307–328, July-September 1998.

[22] G. Margulies and J. N. Aubrun, "Geometric theory of single-gimbal control moment gyro systems," *Journal of the Astronautical Sciences*, vol. 26, no. 2, pp. 159–191, April-June 1978.

[23] T. Yoshikawa, "Analysis and control of robot manipulators with redundancy," in *1st International Symposium on Robotics Research*, Bretton Woods, N.H., August 28 - September 2 1983.

[24] H. S. Oh and S. R. Vadali, "Feedback control and steering laws for spacecraft using single gimbal control moment gyros," *Journal of the Astronautical Sciences*, vol. 39, no. 2, pp. 183–203, April-June 1991.

[25] N. Bedrossian, S. Bhatt, M. Lammers, L. Nguyen, and Y. Zhang, "First ever flight demonstration of zero propellant maneuver attitude control concept," in *AIAA Guidance, Navigation and Control Conference*, Hilton Head S.C., USA, August 20-23 2007.

[26] D. Lemus and H. Vallery, "Towards gyroscopic balance assistance: proof of concept," in *Proceedings of the 36th Annual International Conference of the IEEE Engineering in Medicine and Biology Society*, Chicago, Illonois, USA, August 26-30 2014.

[27] P. Y. Lam, "Gyroscopic stabilization of a kid-size bicycle," in *IEEE 5th International Conference on Cybernetics and Intelligent Systems*, Qindao, China, September 17-19 2011.

[28] J. Lee, S. Han, and J. Lee, "Decoupled dynamic control for pitch and roll axes of the unicycle robot," *IEEE Transactions on Industrial Electronics*, vol. 60, no. 9, pp. 3814–3822, September 2013.

[29] H. B. Brown and Y. Xu, "A single-wheel, gyroscopically stabilized robot," *Proceedings of the IEEE International Conference and Automation*, vol. 4, pp. 3658–3663, 1996.

[30] B. Thornton, T. Ura, Y. Nose, and S. Turnock, "Internal actuation of underwater robots using control moment gyros," in *Oceans Europe*, 2005.

[31] M. A. Peck, M. A. Paluszek, S. J. Thomas, and J. B. Mueller, "Control-moment gyroscopes for joint actuation: A new paradigm in space robotics," in *1st Space Exploration Conference*, Orlando, Florida, USA, January 30 - February 1 2005.

[32] D. Brown, "Control moment gyros as space-robotics actuators," in *AIAA Guidance, Navigation and Control Conference and Exhibit*, Honolulu, Hawaii, USA, August 18-21 2008.

Andrew Berry Andrew Berry received the B.Eng. degree from the University of Victoria, Victoria, Canada in 2012 and the M.Sc. degree in control engineering from the Delft University of Technology (TU Delft), Delft, the Netherlands, in 2015. He is currently a Ph.D. candidate at the TU Delft Robotics Institute. His research interests include nonlinear optimal control, control of unstable systems (particularly human balancing), and rehabilitation robotics.

Daniel Lemus Daniel Lemus received his M.Sc. in mechanical engineering from the Andes University in Bogota, Colombia, in 2011, after which he held positions as a visiting researcher at the Madrid Polytechnic University and the Toyota Motor Europe Technical Center. Since November 2013, he is a Ph.D. candidate at the Delft University of Technology, Delft, the Netherlands, working in research and development of wearable robotics for fall prevention.

Robert Babuška R. Babuška received the M.Sc. (Hons.) degree in control engineering from the Czech Technical University in Prague, in 1990, and the Ph.D. (cum laude) degree from the Delft University of Technology (TU Delft), the Netherlands, in 1997. He has had faculty appointments with the Czech Technical University in Prague and with the Electrical Engineering Faculty, TU Delft. Currently, he is a Professor of Intelligent Control and Robotics at the Delft Center for Systems and Control. He is also the founding director of the TU Delft Robotics Institute. His current research interests include reinforcement learning, neural and fuzzy systems, nonlinear identification, state-estimation, model-based and adaptive control and dynamic multi-agent systems. He has been involved in the applications of these techniques in the fields of robotics, mechatronics, and aerospace.

Heike Vallery Heike Vallery received the Dipl.-Ing. degree in mechanical engineering from RWTH Aachen University, Germany, in 2004, and a doctoral degree from TU Munich, Germany, in 2009. She is currently an Associate Professor at Delft University of Technology. Her research interests include the areas of bipedal locomotion, compliant actuation, and rehabilitation robotics. She has published more than 50 peer-reviewed publications and received diverse awards and fellowships, such as the 1st prize of the euRobotics Technology Transfer Award 2014 and an NWO Vidi in 2016.